Contents lists available at ScienceDirect

# Materials Today Bio

# Endogenus chondrocytes immobilized by G-CSF in nanoporous gels enable repair of critical-size osteochondral defects

Shangkun Tang [a,1], Ruinian Zhang [a,1], Hanying Bai [b], Rui Shu [b,c], Danying Chen [b], Ling He [b], Ling Zhou [d], Zheting Liao [b], Mo Chen [b], Fuxing Pei [a], Jeremy J. Mao [b,e,f,**], Xiaojun Shi [a,*]

[a] Orthopedic Research Institute, Department of Orthopedics, West China Hospital, Sichuan University, Chengdu, 610041, China
[b] Center for Craniofacial Regeneration, Columbia University, New York, NY, 10032, USA
[c] West China School/Hospital of Stomatology, Sichuan University, Chengdu,610041, China
[d] College of Polymer Science and Engineering, State Key Laboratory of Polymer Materials Engineering, Sichuan University, Chengdu, 610041, China
[e] Department of Biomedical Engineering, Columbia University, New York, NY, USA
[f] Department of Pathology and Cell Biology, Columbia University, New York, NY, USA

## ARTICLE INFO

## ABSTRACT

Injured articular cartilage is a leading cause for osteoarthritis. We recently discovered that endogenous stem/progenitor cells not only reside in the superficial zone of mouse articular cartilage, but also regenerated heterotopic bone and cartilage *in vivo*. However, whether critical-size osteochondral defects can be repaired by pure induced chemotatic cell homing of these endogenous stem/progenitor cells remains elusive. Here, we first found that cells in the superficial zone of articular cartilage surrounding surgically created $3 \times 1$ mm defects in explant culture of adult goat and rabbit knee joints migrated into defect-filled fibrin/hylaro1nate gel, and this migration was significantly more robust upon delivery of exogenous granulocyte-colony stimulating factor (G-CSF). Remarkably, G–CSF–recruited chondrogenic progenitor cells (CPCs) showed significantly stronger migration ability than donor-matched chondrocytes and osteoblasts. G–CSF–recruited CPCs robustly differentiated into chondrocytes, modestly into osteoblasts, and barely into adipocytes. *In vivo*, critical-size osteochondral defects were repaired by G–CSF–recruited endogenous cells postoperatively at 6 and 12 weeks in comparison to poor healing by gel-only group or defect-only group. ICRS and O'Driscoll scores of articular cartilage were significantly higher for both 6- and 12-week G-CSF samples than corresponding gel-only and defect-only groups. Thus, endogenous stem/progenitor cells may be activated by G-CSF, a Food and Drug Administration (FDA)-cleared bone-marrow stimulating factor, to repair osteochondral defects.

## 1. Introduction

Articular cartilage injuries are among leading causes for osteoarthritis [1–3]. Current therapeutic interventions including non-specific drugs, microfracture, autologous or allogeneic graft transplantation and cell transplantation are associated with different levels of clinical success but nonetheless are limited by poor quality of repaired tissue, incomplete articular surface coverage, defect re-occurrence or donor-site morbidity [4–9]. Articular cartilage is among the most recalcitrant tissues for self repair [6,9–11]. Robust effort to repair articular cartilage defects using cell-based therapies has primarily focused on transplantation of *ex vivo* cultivated cells [12–18]. Despite various levels of success of experimental studies, *ex vivo* cell culture followed by cell transplantation has encountered an array of clinical difficulties including low cell yield, culture-induced phenotypic alteration and poor *in vivo* cell survival, in addition to regulatory challenges such as cell contamination and cell fate uncertainty [10,11,19–21]. Except for universal donor cells, donor-site morbidity remains undesirable for surgeons or patients.

Hyaluronic acid (HA) is a natural ingredient of synovial fluid, which

is an important composition for joint lubricant and is also used as commonplace intra-articular injection medicine for early-to-mid stage osteoarthritis treatment. Meanwhile, its high biocompatibility and hydrophilic properties make it an appropriate material for biological scaffold and drug delivery. Numerous studies have chosen HA as the key component of scaffold for tissue engineering and regenerative medicine [22–26]. However, HA alone can't convert into solid state gel in order to fill the irregular osteochondral defect, thus HA must be combined with other materials. Fibrin is another natural component in mammals. It depends on the combination of fibrinogen and thrombin and plays an important role in the clotting mechanism, serving as the framework for blood clots. These biochemical characteristics mean it can be used as an injectable, high biocompatibility gel with rapid formation. Therefore, we attempted to integrate these two biological materials and finally got Fibrin/HA hydrogel. The rapid formation of Fibrin/HA hydrogel in situ can fill any irregular osteochondral defect perfectly, and the low degradation rate ensures that there should be plenty of time for tissue repair. The histological origin of the Fibrin/HA hydrogel suggested that it can offer a supportive environment encouraging cell growth, migration, adhesion and differentiation, thereby facilitating tissue repair and regeneration [27,28]. Therefore, the strategic selection of Fibrin/HA hydrogel as a delivery vehicle for special drug is aimed at maximizing its benefits in osteochondral repair by leveraging the natural properties of the hydrogel to create an optimal environment for tissue regeneration, indicating that it is not merely a delivery vehicle, but an integral part of the regenerative process [29].

Previous work has identified progenitor cells in healthy articular cartilage and end-stage osteoarthritis patients [30–32]. Chondrogenic progenitor cells (CPCs) have been characterized as cartilage precursor cells with strong chondrogenic and migratory potential [31–34]. However, whether pure induced chemotactic cell homing of CPCs can repair critical-size osteochondral defects has been elusive. We recently found that adult endogenous stem/progenitor cells not only resided in the superficial zone of mouse articular cartilage via lineage tracing from E16.5–16 weeks, but also regenerated heterotopic bone and cartilage *in vivo* [35]. We further showed that total articular cartilage and partial meniscus injuries were regenerated by host endogenous cells, without cell transplantation [35–37]. Tissue repair by activation of endogenous cells, as opposed to cell transplantation, requires discovery of novel or existing factors that not only induce cell migration, but also promote cell differentiation. Here, we exploited the chemotactic and chondrogenic potential of granulocyte-colony stimulating factor (G-CSF), which was cleared by Food and Drug Administration (FDA) for stimulating bone marrow cell mobilization in non-Hodgkin's lymphoma and multiple myeloma patients [38,39].

## 2. Materials and methods

### 2.1. Explant harvest and cartilage defect

Freshly isolated stifle joints from adult male goats (15–24 months old) obtained from a local slaughter house were incised into $15 \times 15 \times 3$ mm osteochondral explants with intact articular surface from the most convex portion of the tibial plateau. The explants were rinsed in PBS and cultured in DMEM supplemented with 10 % fetal bovine serum, and 50-µg/ml L-ascorbate and 3 % Antibiotic-Antimycotic (Gibco, El Paso, TX, USA). Following 2-day culture, osteochondral defects ($3 \times 1$ mm; diameter $\times$ height) were isolated by mechanical punch, and cultured overnight. Similarly, same size osteochondral defects ($3 \times 1$ mm; diameter $\times$ height) in osteochondral explants of adult rabbits were created. Empty defects were used as blank control. Fibrin/HA gel without G-CSF and Fibrin/HA gel with G-CSF in media were used as a negative control.

### 2.2. Fibrin/hyaluronate hydrogel fabrication and release kinetics

A total of 50 mg/ml fibrinogen (Sigma, St. Louis, MO, USA) was thoroughly mixed with 10 mg/ml hyaluronic acid (HA) (WedMD, New York, NY, USA) and 100 units/ml Thrombin (Sigma) with or without 5-µg/ml G-CSF (Sigma) at a ratio of 7:5 at room temperature. The final concentrations of fibrinogen, HA, thrombin, and G-CSF were 25 mg/ml, 2.5 mg/ml, 16 units/ml and 200 ng/ml, respectively. The protein release kinetics of G-CSF were determined with the use of a previously reported protocol [40]. Briefly, each Fibrin/HA gel was placed in a well of a 24-well plate with 400 µl of DPBS, and then cultured at 37 °C. Supernatants were collected at each time point (days 2, 4, 6, 8, 10, 12, and 14). DPBS (400 µl) was added to replenish each well and samples were placed back for cultivation until the next time point. Enzyme-linked immunosorbent assay was used for quantification, in accordance with the manufacturer's instructions (Sigma).

### 2.3. Rheological analysis

To analyze the gelation kinetics of fibrin/HA hydrogel, a certain volume of Fibrinogen (35 mg/ml)/HA(5 mg/ml) mixed solution before or after the addition of thrombin (250 unit/g) solution at volume ratio of 5:1 was placed between the plate and probe of rheometer (AR2000EX, TA instrument, USA). The storage modulus ($G'$) and loss modulus ($G''$) were recorded in a time sweep mode (strain: 1 %; frequency: 1 Hz). To evaluate the dynamic mechanical property of fibrin/HA hydrogel, the viscoelastic modulus of the fibrinogen/HA solution and fibrin/HA hydrogel was determined in a frequency sweep mode (strain: 1 %, frequency: 0.1–100 rad/s).

### 2.4. Morphological analysis

The physical morphology of the fibrin/HA hydrogel was analyzed using a scanning electron microscope (Quanta 250 FEG, FEI Inc, USA) at an accelerating voltage of 5 kV.

### 2.5. Chemical structure analysis

The chemical structures of the fibrin/HA hydrogel were analyzed using a FTIR spectrometer (Nicolet 6700, Nicolet Instrument Company, USA) in the attenuated total reflectance mode. All spectra were recorded from 4000 to 500 cm−1 with a spectral resolution of 4 cm−1 and 32 scans. The thermal stability of fibrin/HA hydrogel was studied using a thermogravimetric analyzer (TGA2, Mettler Toledo Inc., USA). Test was conducted with a sample weight of 5–8 mg, N2 flow rate of 20 mL/min, and the heating rate of 10 °C/min from 35 to 800 °C.

### 2.6. Mechanical properties analysis

The compressive properties of fibrin hydrogel were analyzed using an mechanical testing instrument (mode 5967, INSTRON Inc, USA) equipped with a load cell of 500 N at 25 °C. Each sample had a cylinder shape with a diameter of 15 mm and a height of 10 mm. The speed of compressing was set to be 2 mm/min. Mechanical properties of regenerated cartilage were determined with the use of our previously reported protocol [41]. Briefly, Cylindrical osteochondral plugs (5·05 [SD 0·50] $\times$ 5·10 [0·32] mm$^2$) were punched from native and G–CSF–regenerated cartilage samples 3 months after G–CSF–contained fibrin/HA gel implantation. Then we did compressive and shear tests using an Electro-Force BioDynamic Tester (Bose, Eden Prairie, MN, USA). Compressive testing was done under 10 % cyclic strain at 2 Hz, and shear testing with 3 % sinusoidal strain under 10 % compressive strain at 2 Hz. The Complex Compressive Modulus (E*), often used in dynamic mechanical analysis, denotes a material's total resistance to deformation under cyclic loading. It comprises both the Storage Modulus (E′), which is the energy stored during deformation and represents the material's stiffness,

and the Loss Modulus (E″), the energy lost as heat during a loading cycle indicative of the material's ability to dampen vibrations. Similarly, the Complex Shear Modulus (G*) gauges the total resistance to shear deformation when a material undergoes cyclic shear loading. It includes the Shear Storage Modulus (G′), which reflects the energy stored during shear deformation, and the Shear Loss Modulus (G″), representing the energy dissipated as heat during a shear loading cycle. Together, these moduli provide comprehensive information about a material's elastic and viscous responses under different types of loading. We characterised dynamic compressive properties as E*, E′, and E″, and dynamic shear properties as G*, G′, and G".

### 2.7. Cell isolation

Explants were stained with 1-mM calcein acettoxymethylester (calcein AM) and 1-mM ethidium homodier-2 (Invitrogen, New York, NY, USA) to appreciate cell viability. Confocal microscopy was performed on harvested articular cartilage samples using Nikon Ti Eclipse inverted microscope (Nikon, Melville, NY, NSA) [42]. Cells were isolated from hydrogel that filled surgically created articular cartilage defects following 1-, 7- and 14-day culture by digestion with type I collagenase (Gibco) at 3 mg/ml per previous methods [19]. Chondrocytes were isolated from donor-matched rabbit articular cartilage adjacent to surgically created defects by surgical mincing and digestion with 3-mg/ml type II collagenase (Gibco). Osteoblasts were isolated by donor-matched subchondral bone by surgical mincing and digestion with 3-mg/ml type I collagenase (Gibco). Cells were cultured in DMEM with 10 % fetal bovine serum supplemented with 1 % Antibiotic-Antimycotic (Gibco), with medium change every 2 days. Passage 1 (p1) cells were used for all *in vitro* experiments.

### 2.8. Cell differentiation

Isolated cells that migrated into hydrogel from articular cartilage were differentiated into osteogenic, chondrogenic and adipogenic lineages. A total of $1 \times 10^5$ migrated cells were seeded in 6-well plates and induced to differentiate in osteogenic, chondrogenic and adipogenic differentiation kits (Gibco). Alizarin Red S was used for osteogenesis; Alcian Blue was used for chondrogenesis; Oil Red O was used for adipogenesis evaluation, all at day 14.

### 2.9. Cell migration

Cell migration was evaluated using 8-μm pore Transwell (Corning, Titterboro, NJ, USA). Trypsinized CPCs, chondrocytes and osteoblasts ($1 \times 10^5$ cells in serum-free medium) were seeded in the upper chamber. Following 24-hr cell starvation, 200 ng/ml G-CSF with or without 1 % serum was added to Transwell's lower chamber. Following 12-hr incubation at 37 °C and 5 % $CO_2$, migrated cells were digested with 0.25 % trypsinase and counted.

### 2.10. FACS analysis

Cells were suspended in 4 °C PBS with fluorescence-coupled antibodies on ice for 30 min and analyzed on a FACS Calibur (BD Biosciences, San Jose, CA, USA), with data analyzed using FlowJo 7.6.

### 2.11. Quantitative real-time PCR

Total RNA was isolated using Trizol (Invitrogen, New York, NY, USA) per manufacturer instructions. cDNA synthesis was performed with random hexamerprimers using iScript™ cDNA Synthesis Kit (Bio-Rad). mRNA was measured by quantitative real-time PCR using SYBR method with 10 mL of SYBR® Green PCR Master Mix(Applied Biosystems), 0.5 μM of each 5′ and 3' primer, 4 μL of sample and H2O to a final volume of 20 μL for 45 cycles with a denaturation at 95 °C for 5 s, annealing and

extension at 60 °C for 34 s. SYBR green fluorescence was measured to determine the amount of double-stranded DNA. All primers were listed in Supplemental Table 1.

### 2.12. Immunofluorescence

Primary cells were transferred to 96-well plates and incubated with primary antibodies for 12 h in the dark, followed by secondary fluorescence-coupled antibodies for 1 h in dark. Two washing steps with PBS and DAPI staining were performed thereafter.

### 2.13. Histological and immunohistochemical evaluation

Explants and *in vivo* tissues were fixed by 10 % formalin for 24 h and decalcified with 0.5-M EDTA (Boston Bioproducts, Boston, MA, USA) for 2 weeks. Hematoxilin and eosin or antibody staining was performed using paraffin-embedded sections.

### 2.14. In vivo animal model

The male rabbits were anesthetized by intravenous injection of 20 % ethyl carbamate (5 ml/kg). The knee joint was opened through an anterior midline skin incision with a medial para-patellar approach, and the patella was dislocated laterally. Critical-size osteochondral defects in the weight-bearing region of the medial femoral condyle (5 × 2 mm; diameter and depth) were created with a corneal trephine. In all rabbits, the right knees were operated upon, whereas the left knees were not operated. Skin and subcutaneous wounds were closed by suturing layer by layer. All rabbits were allowed for free locomotion postoperatively and had free access to food pellets and water. All rabbits were sacrificed with pentobarbital overdose at 6 or 12 weeks postoperatively. The entire right tibial condyles were fixed in 4 % formaldehyde, embedded in paraffin, and cut in 5-μm sections. A total of sixty adult New-Zealand-White rabbits (6-month-old; weighing ~3 kg) were randomly allocated into 3 groups: Group 1 received empty articular-cartilage defects (n = 20). Group 2 received the same articular-cartilage defects filled with fibrin/HA gel (n = 20). Group 3 received the same articular-cartilage defects filled with fibrin/HA gel incorporating 2 μg/ml G-CSF (n = 20). The hydrogel preparation protocol was the same as previous described and gelled within the defect.

### 2.15. Statistical analysis

All statistical analysis was done with SPSS (version 16, IBM, Armonk, US) and PASS 2005. Power analyses were performed with a significance level of 0.05, effect size of 1.50, and power of 0.08. Effect size and power calculations were based on previous published literature [12]. For normal data distribution, quantitative data for control and treated groups were subjected to one-way ANOVA and post-hoc least significant difference tests. For skewed data, we used non-parametric Kruskal--Wallis tests.

## 3. Results

### 3.1. Fabrication and characterization of the nanoporous gels

The nanoporous gels could be readily formed by thrombin-initiated transformation of fibrinogen to become fibrin fibers, and the addition of HA could form abundant nanofibers within the interpenetrating fibrin fibers, endowing it with more dense pores and higher mechanical strength compared to simple fibrin hydrogel. The viscoelastic storage modulus (G′) and loss modulus (G″) of fibrinogen/HA mixture as functions of time and angular frequency sweep are shown in Fig. 1a. After the addition of thrombin, the G′ starts to increase quickly and much higher than that of the G″, indicating that the gelation happened immediately by forming fibrin network. The fully polymerization was then
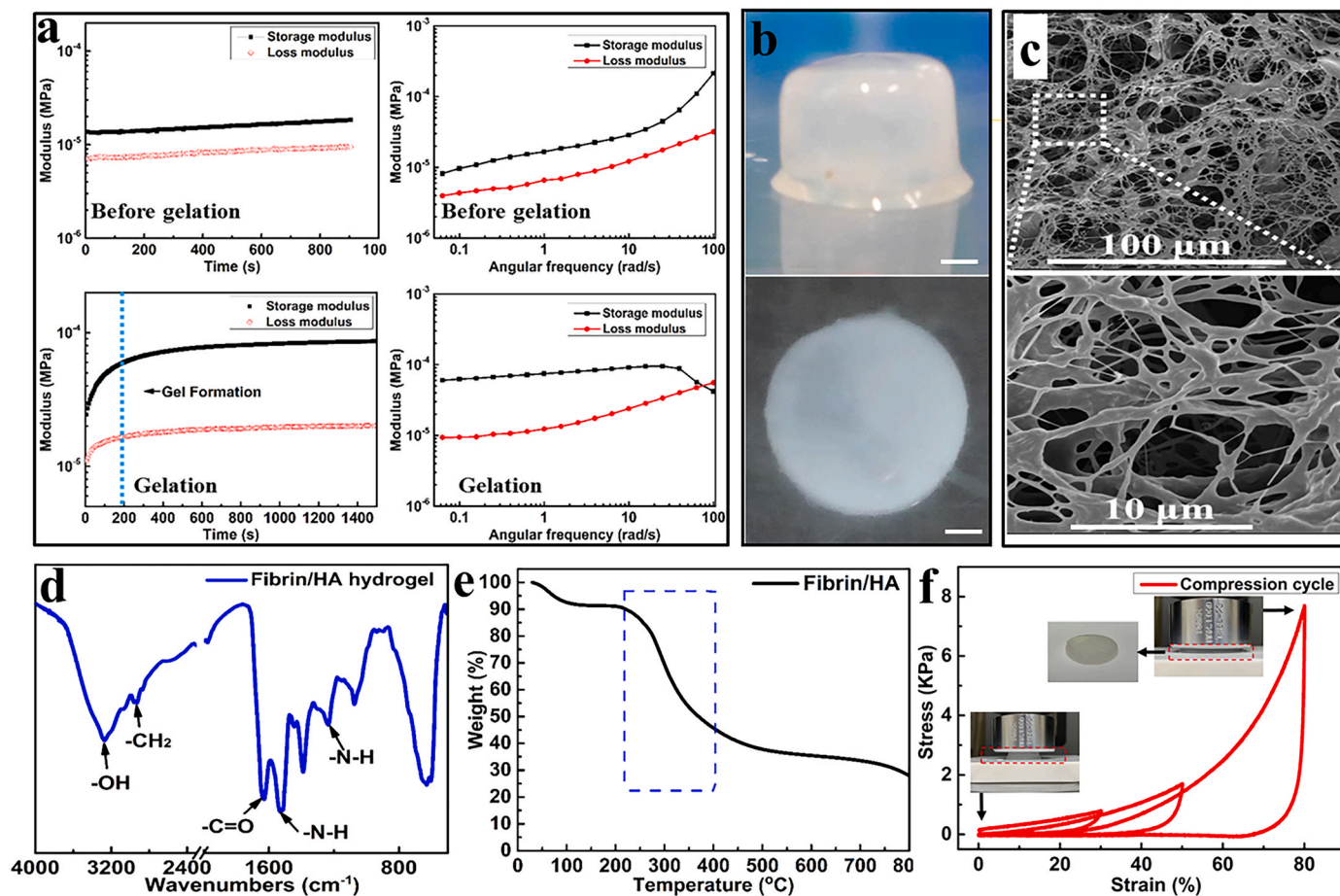
**Fig. 1.** Physical and chemical properties of nanoporous fibrin/HA gel. a:The storage modulus (G′) and loss modulus (G″) of fibrinogen/HA mixture before/after the addition of thrombin as functions of time and angular frequency, respectively. Before the addition of thrombin, the fibrinogen/HA mixture exhibits a typical behavior of predominant viscoelastic fluid wherein the G′ and G″ tends to increase with the increasing of angular frequency. However, both of the G′ and G″ are constant during the time sweep, indicating that no gelation or crosslinking happened in the fibrinogen/HA mixture. After the addition of thrombin, the G′ starts to increase quickly and much higher than that of the G″, indicating that the gelation happened by forming fibrin network. Gross appearance (b), SEM images (c), FTIR curve (d), TGA curve (e) and compressive stress-strain curve (f) of nanoporous fibrin/HA hydrogel. Bar = 1 mm in b.

accomplished within 200 s under physiologic temperatures (37 °C). The obtained nanoporous gels displayed an opaque appearance and a well-defined disk or cylinder shape (Fig. 1b), which also showed typical solid-like viscoelastic behavior proved by the independence of G′ and G″ in lower angular frequency (<50 rad/s). Scanning electron microscopy images showed that the HA nanofiber network was fully distributed within the fibrin fibers (Fig. 1c). The multi-scale network structure not only allowed the cells to attach and migrate both along the surface and within the gels, but also facilitated the transports of nutrients for cell metabolism.

The FTIR analysis of fibrin/HA hydrogel showed that the nanoporous gels exhibited a very similar profile of fibrin protein with characteristic bands in the regions of 1630 cm-1, 1535 cm-1 and 1235 cm-1, which were corresponding to typical of N–H amide III, N–H amide II and C=O amide I, respectively. The vibration deformations of –CH2 at around 2900 cm-1 and –OH at around 3260 cm-1 are also observed. It is noted that the typical peaks of HA are not observed due to its low loadings and functional groups similar to fibrin (Fig. 1d). The TGA test for the thermal stability of fibrin/HA composite showed the major degradation temperature were between 220 and 400 °C (Fig. 1e). Compression measurements for mechanical properties were performed on fibrin/HA hydrogel at compression strain of 30 %, 50 % and 80 %, respectively. As shown in Fig. 1f, the nanoporous gels exhibited typical stress-stain behavior of hydrogels whose compression stress increased non-linearly along with the increased strain. We further profiled the compression

strengths are ca. 0.6, 1.5 and 7.2 KPa, respectively at 30 %, 50 % and 80 % of strain without structural failure (Fig. 1f). These data suggest that fibrin/HA hydrogels are easy to fabricate, and the nanoporous gels contained the solid-like viscoelastic behavior with certain mechanical strength. Although the mechanical strength is much lower than that of cartilage, the fibrin/HA hydrogels may be effective carrier of drug and gene for induced cell-homing for cartilage injury repair.

### 3.2. Spatiotemporally released G-CSF bound to receptors and maintained cell viability

We profiled G-CSF receptor expression in cartilage cells by immunohistochemistry and found robust G-CSF receptor expression among not only superficial zone cells but also deeper zone cells (Fig. 2a and b). Immunofluorescence staining also demonstrated intense G-CSF receptor expression among CPCs and chondrocytes. Contrastingly, CD44 is only positive for CPCs (Fig. 2c). These data laid a theoretical foundation for G-CSF concentration gradient releasing within biological scaffold induced cartilage cells migration to articular cartilage defect without exogenous cell transplantation for osteochondral defect repair.

Nanoporous fibrin/HA gel fabricated from 50 mg/ml fibrinogen with 10 mg/ml hyaluronate and 100 units/ml Thrombin served as a scaffold for surgically created articular cartilage defect as shown in Fig. 2d. After injection of mixed solution into the defect and full polymerization within 3 min, the nanoporous fibrin/HA gel filled the defect perfectly
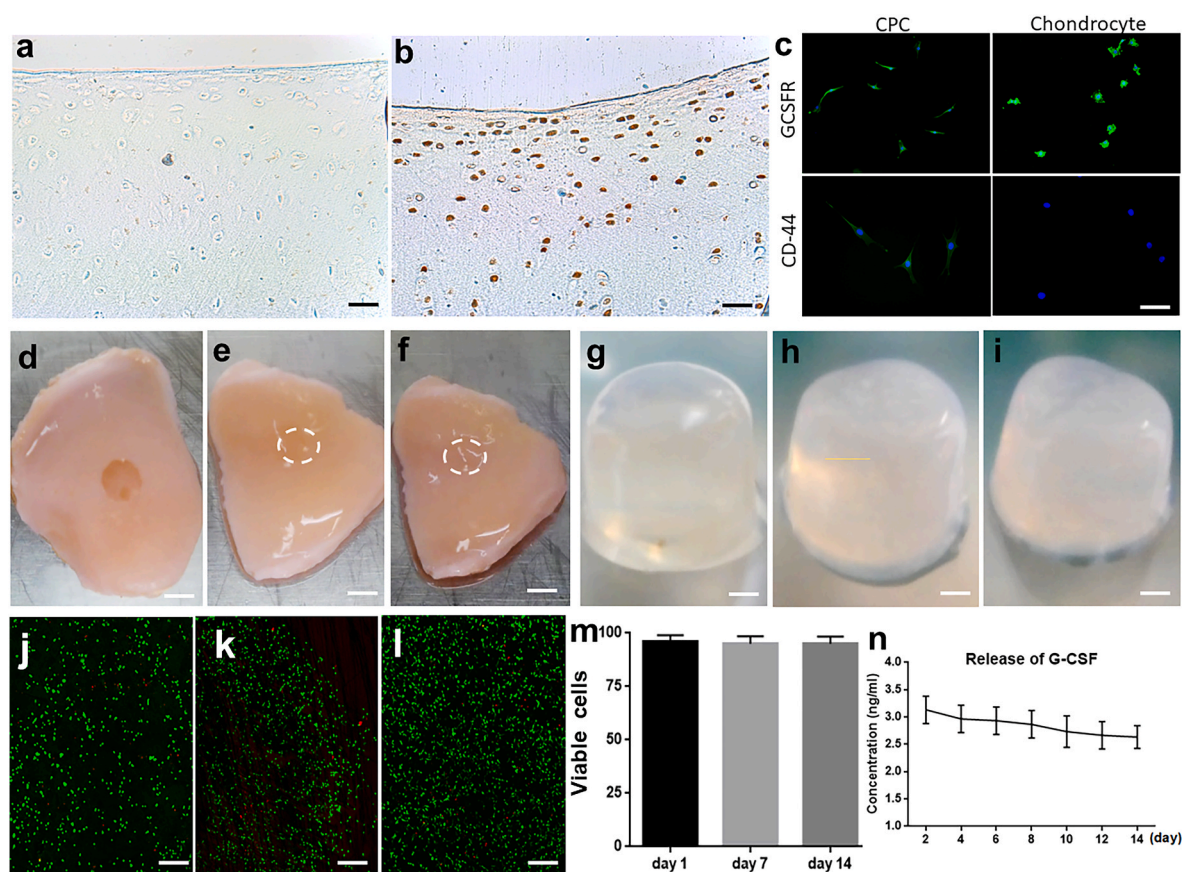
**Fig. 2.** G-CSF receptor assay, Hydrogel implantation, cell viability and G-CSF release kinetics. a,b: G-CSF receptor immunohistochemistry in native articular cartilage of goat knee joint (negative control in a and positive staining in b). c: Immunofluorescence staining for G-CSF receptor and CD44 among CPCs and chondrocyte of goat. d: articular cartilage defect. e,f: Nanoporous fibrin/HA gel filled defects by 1- and 14-days showing complete bridging of the defect by day 14 *in vitro* culture. g: Gross morphology of nanoporous fibrin/HA gel after immediate. h,i: Nanoporous fibrin/HA gel maintained its integrity by 7- and 14-days *in vitro* culture. j–l: Cell viability showing articular chondrocytes encapsulated in fibrin/HA gel at day 1, 7 and 14. Red: dead cells; green: live cells by confocal microscopy with data quantitated in m. n:G-CSF release kinetics from fibrin/HA gel maintained in DPBS shown in n. Bars = 100 μm in a-c; 2 mm in d-i; 500 μm in j-l. (For interpretation of the references to colour in this figure legend, the reader is referred to the Web version of this article.)

without contact gap or other obvious trace and maintained its integrity up to day 14 (Fig. 2e and f). To assess degradation characteristics and cytocompatibility of the biological scaffold, articular chondrocytes were encapsulated in nanoporous fibrin/HA gel with viability evaluated. The nanoporous fibrin/HA gel could maintain its gross appearance upon gross examination in Dulbecco's Modified Eagle's medium (DMEM) up to the tested day 14 (Fig. 2g–i). Confocal microscopy showed few dead cells (red), whereas the great majority of encapsulated cells were alive (green) (Fig. 2j-l). Quantitatively, cell viability was 93.6 ± 1.9 % on day 7 and 93.3 ± 2.2 % on day 14, with no statistically significant decrease in the number of viable cells (Fig. 2m). G-CSF release kinetics from fibrin/HA gel showed continuous extrusion over the tested 14 days (Fig. 2n).

### 3.3. G-CSF immobilized superficial zone cells of injured articular cartilage

For a cartilage defect to heal, cells must be transplanted and/or recruited into the defect. Following creation of osteochondral defects in osteochondral explants of adult goat and rabbit knee joints with or without filling with a fibrin/hyaluronate gel, we first observed whether cells from the surrounding articular cartilage and/or subchondral bone could migrate into the defect. Cell migration was monitored by confocal microscopy at days 1, 7 and 14 (Fig. 3a–i). Few cells migrated into the defect in explants with empty defect or fibrin/hylaronate (fibrin/HA) gel over the observed 14 days (Fig. 3a–f, Supplementary Figs. 1a–f). Similarly, only a few unordered cells migrated into the defect with fibrin/HA

gel with G-CSF in media by day 14 (Supplementary Fig. 1j-l). Contrastingly, cells began to migrate into G–CSF–contained fibrin/HA gel by day 7 (Fig. 3h, Supplementary Fig. 1h), with abundant cells populating the defect area by day 14 (Fig. 3i). Further analysis found that G-CSF migrated cells were primarily from the superficial zone of articular cartilage surrounding the defect at day 7 (Fig. 3j,k,l). Additional H&E stained sections confirmed that G–CSF–immobilized cells were primarily from the superficial zone of articular cartilage (Fig. 3o), and little cell migration in articular cartilage except for the superficial zone (fig. 3m–o). Positive immune-fluorescence staining of PRG4 and GDF5 at day 7 demonstrated that these G-CSF immobilized cells were from the superficial layer of cartilage (Supplementary Fig. 2).

### 3.4. G-CSF immobilized cells are chondrogenic progenitor cells

We further isolated cells that migrated into fibrin/hylaronate gel in the surgically created articular cartilage defects with schematics shown in Fig. 4a–f, and plated the cells as in Fig. 4e, along with articular chondrocytes isolated from adjacent articular cartilage (Fig. 4g) and osteoblasts from subchondral bone (Fig. 4h). G-CSF immobilized cells showed significantly more robust migratory ability upon Transwell assays than native chondrocytes and osteoblast (Fig. 4j and k), and again G-CSF further promoted cell migration (Fig. 4m). Meanwhile, G-CSF immobilized cells isolated from the defects at day 3/7/14 showed no significantly difference in migratory ability upon transwell migration (Supplementary Fig. 3). Given its robust ability to induce chemotaxis,
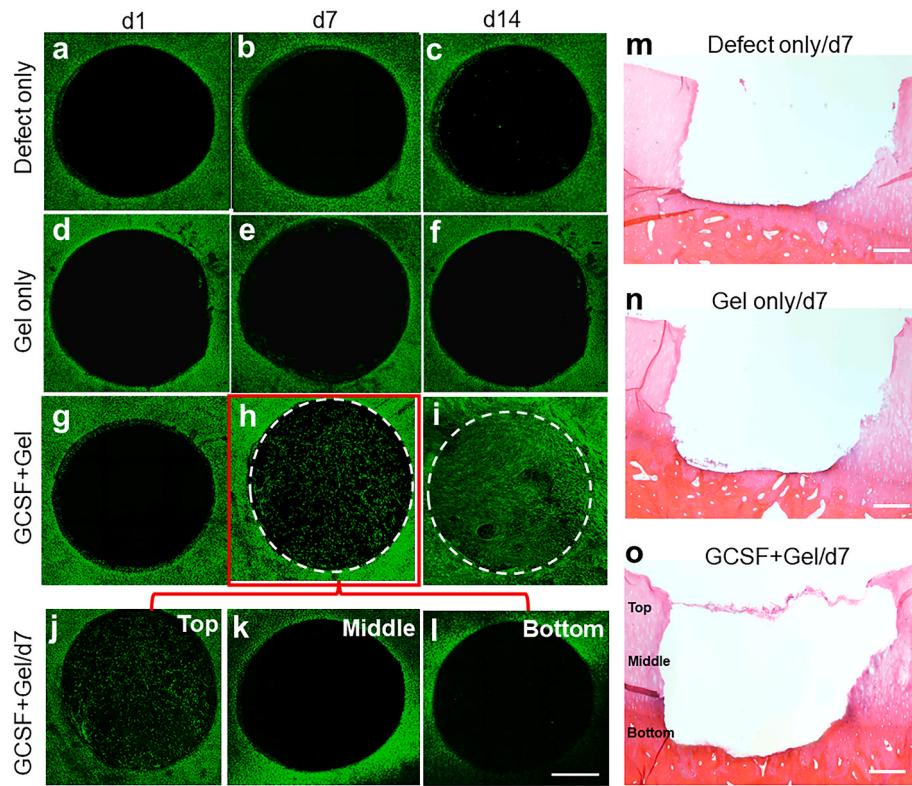
**Fig. 3.** Cell migration from superficial zone of goat articular cartilage. Full-thickness articular cartilage defects ($3 \times 1$ mm$^3$, diameter $\times$ height) were created in the most convex portion of the tibial plateau. a–l: confocal microcopy images showing cell migration or a lack of. a–c: defects only. d–f: defects filled with a fibrin/hylaronate gel. g–i: G–CSF–contained nanoporous fibrin/HA gel at 1, 7 and 14 days, with 7- and 14-day samples showing cell migration. j–l: Top, middle and bottom layer of G–CSF–contained fibrin/HA gel at day 7 showing migration of superficial zone cells, with few cells migrated in middle and bottom zones. m: Defect only sample at day 7. n: fibrin/hylaronate gel only sample at day 7. o: G–CSF–contained gel sample at day 7 showing migration of superficial zone cells. Bars = 1 mm in a-l; 200 μm in m-o.
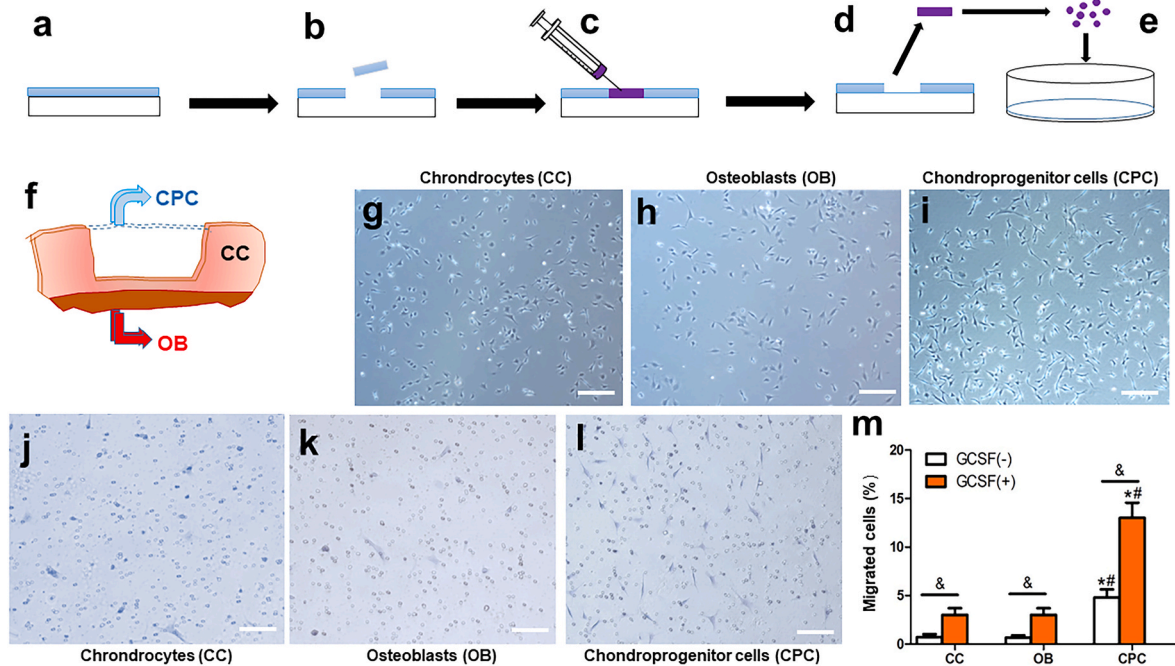


**Fig. 4.** G-CSF immobilized cells show progenitor properties. a–e: Schematics of cartilage defects and cell isolation. f: Isolation of chondrogenic progenitor cells (CPCs), and chondrocytes (CC) from articular cartilage adjacent to surgically created defects and osteoblasts (OB) from subchondral bone. g–i: Plated chondrocytes (CC), osteoblasts (OB) and chondrogenic progenitor cells (CPCs). j–l: Migrated cells of Transwell assay and quantification of % migrated cells (m). &: $p < 0.01$ for within group comparison; *#: $p < 0.01$ from all other groups; n = 6 per group. Bars = 200 μm in j-l.

we profiled G-CSF recruited CPCs by flow cytometry (Fig. 5a–e). G–CSF–positive cells were positive for CD29 (25.9 %), CD44 (97.9 %), CD90 (29.1 %) and CD105 (37 %), but negative for CD45 (<0.2 %) (Fig. 5a–e). We further profiled G-CSF immobilized CPCs with real-time, quantitative PCR and found that CPCs were indeed of precursor phenotype with little expression of RunX2, Sox9, Aggrecan, collagen type II and collagen type X (Fig. 5f–h, j,k), with the exception of a lack of significance differences in collagen type I from donor-matched chondrocytes and osteoblasts (Fig. 5i).

Furthermore, G–CSF–immobilized CPCs showed robust ability to differentiate into chondrocyte-like cells upon Alcian Blue staining and formed Safranin O-positive cell pellets (Fig. 5l-n), and modest ability to differentiate osteoblast-like cells upon Alizarin red staining (Fig. 5o,p), but importantly barely into adipocyte-like cells with Oil-red-O staining (Fig. 5q). These data suggest that G–CSF–immobilized cells were likely not stem cells but rather skeletal progenitors primarily with embedded abilities to differentiate into chondrocytes with reduced and diminished capacity to differentiate into osteoblasts and adipocytes.

### 3.5. Spatiotemporally released G-CSF induced repair of critical-size osteochondral defects

Critical-size osteochondral defects in the weight-bearing region of the medial femoral condyle (5 × 2 mm; diameter and depth) of skeletally mature New Zealand White rabbits (6-month-old; weighing ~3 kg). A total of sixty adult New-Zealand-White rabbits were randomly allocated into 3 groups: Group 1 received empty osteochondral defects (n = 20); Group 2 received fibrin/HA gel (n = 20) in surgically created osteochondral defects; Group 3 received fibrin/HA gel with 200 ng/ml G-CSF (n = 20). Upon sample harvest postoperatively at 6 weeks, insufficient

tissue fill was associated with not only defect samples (Fig. 6a), but also fibrin/HA gel samples (Fig. 6b). Even by week 12, defect-only and gel-only samples still lacked tissue fill (Fig. 6d and e). In contrast, G-CSF immobilized fibrin/HA gel induced tissue fill in surgically created osteochondral defects by 6 weeks (Fig. 6c). By 12 weeks, G-CSF induced repair with semitransparent tissue and smooth articular surface, showing apparent continuity of repair tissue with the surrounding native articular cartilage (Fig. 6f). Immunohistochemistry staining confirmed gross morphological findings. Defect alone samples lacked tissue repair in surgically created osteochondral defects, without Alcian Blue, type II collagen or Safranin O staining, in contrast to positive staining outcome of surrounding articular cartilage (Fig. 6g1, h1, i1, j1 and k1). Similarly, fibrin-HA gel filled samples showed little repair tissue in surgically created osteochondral defects, with little tissue and general absence of Alcian Blue, collagen type II and Safranin O staining (Fig. 6g2, h2, i2, j2 and k2). Contrastingly, osteochondral defects filled with G–CSF–contained fibrin/HA gel showed partial or nearly complete tissue fill with positive staining to Alcian Blue, collagen type II and Safranin O at both 6 weeks (Fig. 6g3, i3 and k3) and 12 weeks (Fig. 6h3, j3 and l3). There appeared to be a qualitative improvement of repaired cartilage-like tissue from 6-week samples (Fig. 6c, g3, i3 and k3) to 12-week samples (Fig. 6f, h3, j3 and l3) upon G-CSF delivery. G-CSF delivery resulted in significantly improved articular cartilage at both 6 and 12 weeks in comparison to both defect along and G–CSF–free fibrin/HA gel groups using modified O'Driscoll scores [43,44] and ICRS scores [6, 43]. These scoring systems take into account various factors, including subchondral bone, cartilage structural integrity, cartilage surface smoothness, cartilage thickness, joint range of motion, and joint stability.

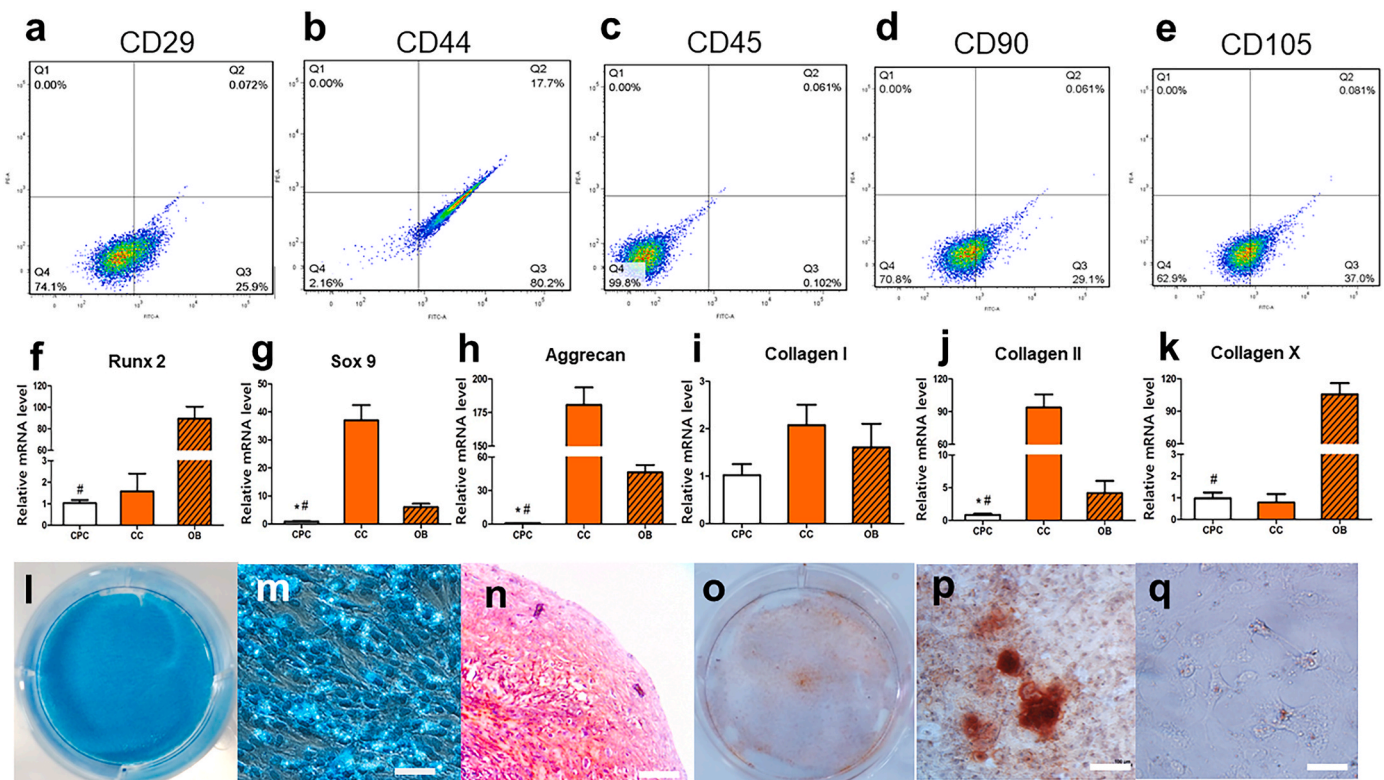3 months after implantation, $|E^*|$, $E'$, and $E''$ of G–CSF–regenerated



**Fig. 5.** Characterization of chondrogenic progenitor cells and differentiation. a–e: G-CSF recruited chondrogenic progenitor cells (CPCs) by flow cytometry showing CD29 (25.9 %), CD44 (97.9 %), CD90 (29.1 %) and CD105 (37 %), but negative for CD45 (<0.2 %). f–k: mRNA expression of Runx2, Sox9, Aggrecan, collagen type I, collagen type II and collagen type X by real-time, quantitative PCR. l,m: Alcian Blue staining and chondrocyte-like cells differentiated from CPCs in chondrogenic medium. n: Safranin O-stained pellet showing chondrogenic differentiation from CPCs in chondrogenic medium. o,p: Modest Alizarin red staining of CPCs in osteogenic medium. q: Little Oil-red-O staining of CPCs in adipogenic medium. Bars = 100 μm. (For interpretation of the references to colour in this figure legend, the reader is referred to the Web version of this article.)
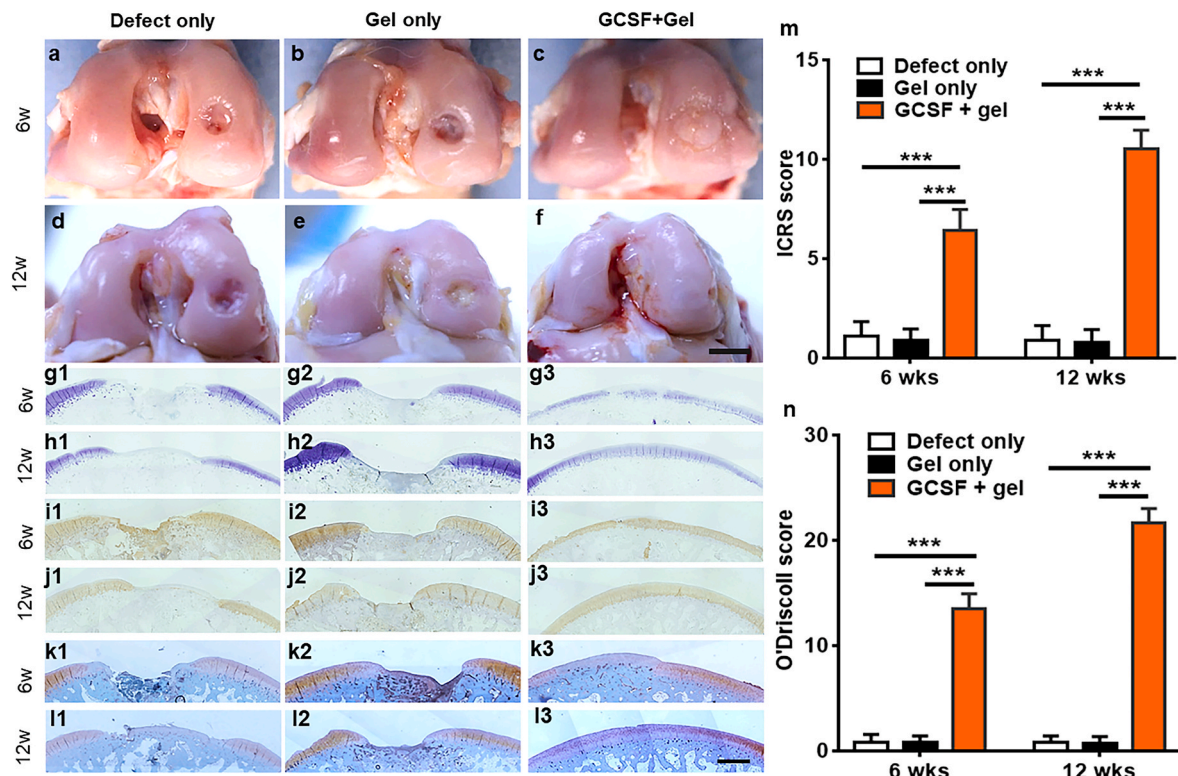
**Fig. 6.** G–CSF–contained nanoporous fibrin/HA hydrogel repaired critical-size, full-thickness osteochondral defects (5 × 2 mm; diameter and depth). Under general anesthesia, the rabbit knee joint was opened to create critical-size, full-thickness articular osteochondral defects in the weight-bearing region of the medial femoral condyle (5 × 2 mm; diameter and depth). a–c: representative 12-wk postoperative samples of defect alone, gel only and G-CSF gel samples. g1-g3; h1-h3: representative 6- and 12-wk postoperative samples of defect alone, gel only and G-CSF gel samples stained with Alcian blue. i1-i3; j1-j3: representative 6- and 12-wk postoperative samples of defect alone, gel only and G-CSF gel samples stained with collagen type II. k1-k3; l1-l3: representative 6- and 12-wk postoperative samples of defect alone, gel only and G-CSF gel samples stained with Safranin O. m, n: ICRS and O'Driscoll scores of articular cartilage performed on 6- and 12-wk harvested samples. ***: $p < 0.01$; n = 10 per group. Bars = 5 mm in a-f; 1 mm in g-l. (For interpretation of the references to colour in this figure legend, the reader is referred to the Web version of this article.)

articular cartilage samples did not differ from those of native articular cartilage, (Supplmentary Fig. 4; n = 5 for all groups). Similarly, |G*| and G' did not differ between native and G–CSF–regenerated cartilage samples, but G" was significantly higher in native cartilage than in G–CSF–regenerated. In general, the dynamic viscoelastic moduli of the G–CSF–regenerated articular cartilage were similar to those of the native articular cartilage samples.

## 4. Discussion

The present findings demonstrate that CPCs are immobilized by G-CSF and gain the ability to repair critical-size osteochondral defects that extend into subchondral bone *in vivo*. In the defect alone group, CPCs are present just as in the G-CSF group, but lack the ability to repair critical-size defects, suggesting that G-CSF is pivotal for recruiting sufficient number of precursors and/or chondrocytes that participate in the observed repair of articular cartilage defects. Our *in vitro* finding of CPC's migratory ability not only is consistent with previous findings in normal and human osteoarthritic cartilage [30–32,45–47], but also extends previous work by showing that G-CSF further immobilizes CPCs, and repairs critical-size osteochondral defects. Previously, G-CSF receptors and signaling have been exploited primarily in the immobilization of monocytes and hematopoietic stem cells [38,39,48,49], leading to disruption of the CXCR4/SDF-1α retention axis by depressing the expression of both receptor and ligands [38,50]. Our finding of G-CSF receptor presence throughout all zones of articular cartilage suggests G-CSF's previously underexplored roles potentially in cartilage repair. In explants, only superficial zone cells including CPCs are

recruited by G-CSF as shown in our findings. *In vivo*, delivered G-CSF ligands probably have bound to G-CSF receptors throughout all zones of articular cartilage. We speculate that G-CSF recruited cells *in vivo* may have derived from all depths of articular cartilage, and perhaps bone marrow, which in totality are responsible for the observed cartilage repair. At first, we thought that our *in vitro* explant data showing recruitment of superficial zone CPCs are contradictory with the probability of *in vivo* data showing cartilage repair perhaps by all zones of cells. *In vitro*, G-CSF recruitment of superficial zone cells may be accounted for by at least two possibilities. First, superficial zone CPCs are more readily recruited than donor-matched chondrocytes and osteoblasts, as shown by our *in vitro* data. *In vivo*, superficial zone CPCs perhaps are the primary cells that are recruited and have differentiated to repair articular-cartilage defects. Alternatively, fibrin/HA gel degradation may not be rapid enough to have allowed G-CSF recruitment of deeper zone cells, perhaps not a strong probability because at least some fibrin/HA gel should have undergone degradation in the observed 14 days *in vitro*.

G-CSF immobilized cells appear to be skeletal progenitors with capacity to differentiate into chondrocytes and osteoblasts, but diminished ability to differentiate into adipocytes, and therefore perhaps are somewhat more lineage-restricted than bone marrow mesenchymal stem cells(MSCs) [30–32,45,51]. Our finding of CPCs' stronger migration capacity than donor-matched chondrocytes, somewhat modest ability to differentiate into osteoblasts and little ability to differentiate into adipocytes suggests that at least some, if not the majority, of repair cells *in vivo* are progenitor cells which may first be recruited into cartilage defects and then differentiate into chondrocytes due to the

delivered G-CSF. The present findings extend previous work by us and others that collectively have shown that endogenous cells, including stem/progenitor cells, may be sufficient to repair tissue or organ defects, without transplantation of ex *vivo* cultivated cells [35–37,48]. G-CSF recruited cells may include not only CPCs, but also bone marrow or synovial-derived MSCs which respond to other growth factors and cytokines [31,32,35–37,52,53]. Additional work is needed to elucidate the sources of homed endogenous cells that have repaired articular cartilage defects.

Repair of critical-size osteochondral defects in skeletally mature rabbits with a 12-weeks follow up is attributed primarily to G-CSF. Despite the claim that rabbit articular cartilage defects may heal spontaneously, our control group shows a lack of healing, suggesting the validity of the present model as a non-healing defect. The presently selected critical-size articular cartilage defects in the weight-bearing area of the femoral condyle serve as relevant reference for several other models with defects in the non-weight-bearing trochlear groove [12,54–56]. Our demonstrated *in vivo* samples are true representative samples with quantitative ICRS and O'Driscoll scores showing overall *in vivo* repair of surgically created articular cartilage defects.

It is important to recognize that our study has several inherent limitations. Our *in vivo* findings are limited by several factors. First, *in vivo* articular cartilage defects are created acutely without fibrosis or scar tissue formation as in focal defects in patients. Second, acute articular cartilage defects, as created in the present study, may elicit acute inflammatory responses which may stimulate repair [52,53,57].

## 5. Conclusion

Within these and other constraints, the present findings suggest that endogenous stem/progenitor cells may be activated by G-CSF, a FDA-cleared bone-marrow stimulating factor, to repair articular-cartilage defects.

## Ethical statement

The animal experiments were conducted following the protocols approved by Sichuan University West China Hospital Animal Ethics Committee using National Institutes of Health guide for the care and use of laboratory animals (NIH Publication No. 8023, revised 1987).

## CRediT authorship contribution statement

**Shangkun Tang:** Conceptualization, Data curation, Investigation, Methodology, Software, Supervision, Writing – original draft, Writing – review & editing. **Ruinian Zhang:** Conceptualization, Data curation, Methodology, Writing – original draft, Writing – review & editing. **Hanying Bai:** Formal analysis, Methodology, Project administration, Software, Visualization. **Rui Shu:** Formal analysis, Methodology, Resources, Software. **Danying Chen:** Formal analysis, Methodology, Resources, Software. **Ling He:** Formal analysis, Resources, Software, Supervision. **Ling Zhou:** Investigation, Methodology, Software. **Zheting Liao:** Methodology, Validation, Visualization. **Mo Chen:** Methodology, Software. **Fuxing Pei:** Investigation, Supervision. **Jeremy J. Mao:** Conceptualization, Funding acquisition, Investigation, Methodology, Project administration, Writing – original draft, Writing – review & editing. **Xiaojun Shi:** Conceptualization, Data curation, Formal

analysis, Funding acquisition, Methodology, Software, Writing – original draft, Writing – review & editing.

## Declaration of competing interest

The authors declare that they have no known competing financial interests or personal relationships that could have appeared to influence the work reported in this paper.

## Data availability

Data will be made available on request.

## Appendix A. Supplementary data

Supplementary data to this article can be found online at https://doi.org/10.1016/j.mtbio.2023.100933.

## References

[1] K. Allen, L. Thoma, Y. Golightly, Epidemiology of osteoarthritis, Osteoarthritis Cartilage 30 (2) (2022) 184–195, https://doi.org/10.1016/j.joca.2021.04.020.

[2] A. Pitsillides, F. Beier, Cartilage biology in osteoarthritis–lessons from developmental biology, Nat. Rev. Rheumatol. 7 (11) (2011) 654–663, https://doi.org/10.1038/nrrheum.2011.129.

[3] J. Quicke, P. Conaghan, N. Corp, G. Peat, Osteoarthritis year in review 2021: epidemiology & therapy, Osteoarthritis Cartilage 30 (2) (2022) 196–206, https://doi.org/10.1016/j.joca.2021.10.003.

[4] G. Deyle, C. Allen, S. Allison, N. Gill, B. Hando, E. Petersen, D. Dusenberry, D. Rhon, Physical therapy versus glucocorticoid injection for osteoarthritis of the knee, N. Engl. J. Med. 382 (15) (2020) 1420–1429, https://doi.org/10.1056/NEJMoa1905877.

[5] C. Ibarra, E. Villalobos, A. Madrazo-Ibarra, C. Velasquillo, V. Martinez-Lopez, A. Izaguirre, A. Olivos-Meza, S. Cortes-Gonzalez, F. Perez-Jimenez, A. Vargas-Ramirez, G. Franco-Sanchez, L. Ibarra-Ibarra, L. Sierra-Suarez, A. Almazan, C. Ortega-Sanchez, C. Trueba, F. Martin, R. Arredondo-Valdes, D. Chavez-Arias, Arthroscopic matrix-assisted autologous chondrocyte transplantation versus microfracture: a 6-year follow-up of a prospective randomized trial, Am. J. Sports Med. 49 (8) (2021) 2165–2176, https://doi.org/10.1177/03635465211010487.

[6] G. Knutsen, J. Drogset, L. Engebretsen, T. Grøntvedt, T. Ludvigsen, S. Løken, E. Solheim, T. Strand, O. Johansen, A randomized multicenter trial comparing autologous chondrocyte implantation with microfracture: long-term follow-up at 14 to 15 years, J Bone Joint Surg AM 98 (16) (2016) 1332–1339, https://doi.org/10.2106/jbjs.15.01208.

[7] H. Oshiba, T. Itsubo, S. Ikegami, K. Nakamura, S. Uchiyama, H. Kato, Results of bone peg grafting for capitellar osteochondritis dissecans in adolescent baseball players, Am. J. Sports Med. 44 (12) (2016) 3171–3178, https://doi.org/10.1177/0363546516658038.

[8] T. Saris, T. de Windt, E. Kester, L. Vonk, R. Custers, D. Saris, Five-Year outcome of 1-stage cell-based cartilage repair using recycled autologous chondrons and allogenic mesenchymal stromal cells: a first-in-human clinical trial, Am. J. Sports Med. 49 (4) (2021) 941–947, https://doi.org/10.1177/0363546520988069.

[9] L. Acevedo Rua, M. Mumme, C. Manferdini, S. Darwiche, A. Khalil, M. Hilpert, D. Buchner, G. Lisignoli, P. Occhetta, B. von Rechenberg, M. Haug, D. Schaefer, M. Jakob, A. Caplan, I. Martin, A. Barbero, K. Pelttari, Engineered nasal cartilage for the repair of osteoarthritic knee cartilage defects, Sci. Transl. Med. 13 (609) (2021), https://doi.org/10.1126/scitranslmed.aaz4499 eaaz4499.

[10] A. Gobbi, G. Whyte, One-stage cartilage repair using a hyaluronic acid-based scaffold with activated bone marrow-derived mesenchymal stem cells compared with microfracture: five-year follow-up, Am. J. Sports Med. 44 (11) (2016) 2846–2854, https://doi.org/10.1177/0363546516656179.

[11] A. Clavé, J. Potel, E. Servien, P. Neyret, F. Dubrana, E. Stindel, Third-generation autologous chondrocyte implantation versus mosaicplasty for knee cartilage injury: 2-year randomized trial, J. Orthop. Res. 34 (4) (2016) 658–665, https://doi.org/10.1002/jor.23152, official publication of the Orthopaedic Research Society.

[12] W. Fu, C. Zhou, J. Yu, A new source of mesenchymal stem cells for articular cartilage repair: MSCs derived from mobilized peripheral blood share similar biological characteristics in vitro and chondrogenesis in vivo as MSCs from bone marrow in a rabbit model, Am. J. Sports Med. 42 (3) (2014) 592–601, https://doi.org/10.1177/0363546513512778.

[13] M. Deng, S. Wei, T. Yew, P. Lee, T. Yang, H. Chu, S. Hung, Cell therapy with G-CSF-mobilized stem cells in a rat osteoarthritis model, Cell Transplant. 24 (6) (2015) 1085–1096, https://doi.org/10.3727/096368914x680091.

[14] L. Keller, L. Pijnenburg, Y. Idoux-Gillet, F. Bornert, L. Benameur, M. Tabrizian, P. Auvray, P. Rosset, R. María Gonzalo-Daganzo, E. Gómez Barrena, L. Gentile, N. Benkirane-Jessel, Preclinical safety study of a combined therapeutic bone wound dressing for osteoarticular regeneration, Nat. Commun. 10 (1) (2019) 2156, https://doi.org/10.1038/s41467-019-10165-5.

[15] I. Erickson, S. Kestle, K. Zellars, M. Farrell, M. Kim, J. Burdick, R. Mauck, High mesenchymal stem cell seeding densities in hyaluronic acid hydrogels produce engineered cartilage with native tissue properties, Acta Biomater. 8 (8) (2012) 3027–3034, https://doi.org/10.1016/j.actbio.2012.04.033.

[16] M. Bhattacharjee, J. Escobar Ivirico, H. Kan, S. Shah, T. Otsuka, R. Bordett, M. Barajaa, N. Nagiah, R. Pandey, L. Nair, C. Laurencin, Injectable amnion hydrogel-mediated delivery of adipose-derived stem cells for osteoarthritis treatment, Proc. Natl. Acad. Sci. U. S. A. 119 (4) (2022), https://doi.org/10.1073/pnas.2120968119.

[17] S. Tan, Y. Kwan, W. Neo, J. Chong, T. Kuek, J. See, K. Wong, W. Toh, J. Hui, Intra-articular injections of mesenchymal stem cells without adjuvant therapies for knee osteoarthritis: a systematic review and meta-analysis, Am. J. Sports Med. 49 (11) (2021) 3113–3124, https://doi.org/10.1177/0363546520981704.

[18] Y. Park, C. Ha, J. Kim, W. Han, J. Rhim, H. Lee, K. Kim, Y. Park, J. Chung, Single-stage cell-based cartilage repair in a rabbit model: cell tracking and in vivo chondrogenesis of human umbilical cord blood-derived mesenchymal stem cells and hyaluronic acid hydrogel composite, Osteoarthritis Cartilage 25 (4) (2017) 570–580, https://doi.org/10.1016/j.joca.2016.10.012.

[19] Y. Moon, M. Patel, S. Um, H. Lee, S. Park, S. Park, S. Cha, B. Jeong, Folic acid pretreatment and its sustained delivery for chondrogenic differentiation of MSCs, J. Contr. Release : official journal of the Controlled Release Society 343 (2022) 118–130, https://doi.org/10.1016/j.jconrel.2022.01.018.

[20] D. Prockop, Repair of tissues by adult stem/progenitor cells (MSCs): controversies, myths, and changing paradigms, Molecular therapy, the journal of the American Society of Gene Therapy 17 (6) (2009) 939–946, https://doi.org/10.1038/mt.2009.62.

[21] T. de Windt, L. Vonk, I. Slaper-Cortenbach, M. van den Broek, R. Nizak, M. van Rijen, R. de Weger, W. Dhert, D. Saris, Allogeneic mesenchymal stem cells stimulate cartilage regeneration and are safe for single-stage cartilage repair in humans upon mixture with recycled autologous chondrons, Stem Cell. 35 (1) (2017) 256–264, https://doi.org/10.1002/stem.2475.

[22] M. Hemshekhar, R.M. Thushara, S. Chandranayaka, L.S. Sherman, K. Kemparaju, K.S. Girish, Emerging roles of hyaluronic acid bioscaffolds in tissue engineering and regenerative medicine, Int. J. Biol. Macromol. 86 (2016) 917–928, https://doi.org/10.1016/j.ijbiomac.2016.02.032.

[23] R. Dimatteo, N.J. Darling, T. Segura, In situ forming injectable hydrogels for drug delivery and wound repair, Adv. Drug Deliv. Rev. 127 (2018) 167–184, https://doi.org/10.1016/j.addr.2018.03.007.

[24] M.N. Collins, C. Birkinshaw, Hyaluronic acid based scaffolds for tissue engineering–a review, Carbohydr. Polym. 92 (2) (2013) 1262–1279, https://doi.org/10.1016/j.carbpol.2012.10.028.

[25] K. Flégeau, A. Puiggali-Jou, M. Zenobi-Wong, Cartilage tissue engineering by extrusion bioprinting utilizing porous hyaluronic acid microgel bioinks, Biofabrication 14 (3) (2022), https://doi.org/10.1088/1758-5090/ac6b58.

[26] C.C.L. Schuurmans, M. Mihajlovic, C. Hiemstra, K. Ito, W.E. Hennink, T. Vermonden, Hyaluronic acid and chondroitin sulfate (meth)acrylate-based hydrogels for tissue engineering: synthesis, characteristics and pre-clinical evaluation, Biomaterials 268 (2021) 120602, https://doi.org/10.1016/j.biomaterials.2020.120602.

[27] E. Oh, J.E. Oh, J. Hong, Y. Chung, Y. Lee, K.D. Park, S. Kim, C.O. Yun, Optimized biodegradable polymeric reservoir-mediated local and sustained co-delivery of dendritic cells and oncolytic adenovirus co-expressing IL-12 and GM-CSF for cancer immunotherapy, J. Contr. Release 259 (2017) 115–127, https://doi.org/10.1016/j.jconrel.2017.03.028.

[28] Q. Xu, J. Torres, M. Hakim, P. Babiak, P. Pal, C. Battistoni, M. Nguyen, A. Panitch, L. Solorio, J. Liu, Collagen- and hyaluronic acid-based hydrogels and their biomedical applications, Materials science & engineering, R. Rep. : a review journal 146 (2021), https://doi.org/10.1016/j.mser.2021.100641.

[29] J. Wen, B. Hou, W. Lin, F. Guo, M. Cheng, J. Zheng, P. He, W. Ji, 3D-printed hydrogel scaffold-loaded granulocyte colony-stimulating factor sustained-release microspheres and their effect on endometrial regeneration, Biomater. Sci. 10 (12) (2022) 3346–3358, https://doi.org/10.1039/d2bm00109h.

[30] S. Alsalameh, R. Amin, T. Gemba, M. Lotz, Identification of mesenchymal progenitor cells in normal and osteoarthritic human articular cartilage, Arthritis Rheum. 50 (5) (2004) 1522–1532, https://doi.org/10.1002/art.20269.

[31] S. Koelling, J. Kruegel, M. Irmer, J. Path, B. Sadowski, X. Miro, N. Miosge, Migratory chondrogenic progenitor cells from repair tissue during the later stages of human osteoarthritis, Cell Stem Cell 4 (4) (2009) 324–335, https://doi.org/10.1016/j.stem.2009.01.015.

[32] D. Seol, D. McCabe, H. Choe, H. Zheng, Y. Yu, K. Jang, M. Walter, A. Lehman, L. Ding, J. Buckwalter, J. Martin, Chondrogenic progenitor cells respond to cartilage injury, Arthritis Rheum. 64 (11) (2012) 3626–3637, https://doi.org/10.1002/art.34613.

[33] Y. Yu, M. Brouillette, D. Seol, H. Zheng, J. Buckwalter, J. Martin, Use of recombinant human stromal cell-derived factor 1α-loaded fibrin/hyaluronic acid hydrogel networks to achieve functional repair of full-thickness bovine articular cartilage via homing of chondrogenic progenitor cells, Arthritis Rheumatol. 67 (5) (2015) 1274–1285, https://doi.org/10.1002/art.39049.

[34] Y. Jiang, R. Tuan, Origin and function of cartilage stem/progenitor cells in osteoarthritis, Nat. Rev. Rheumatol. 11 (4) (2015) 206–212, https://doi.org/10.1038/nrrheum.2014.200.

[35] M. Embree, M. Chen, S. Pylawka, D. Kong, G. Iwaoka, I. Kalajzic, H. Yao, C. Shi, D. Sun, T. Sheu, D. Koslovsky, A. Koch, J. Mao, Exploiting endogenous fibrocartilage stem cells to regenerate cartilage and repair joint injury, Nat. Commun. 7 (2016) 13073, https://doi.org/10.1038/ncomms13073.

[36] C. Lee, S. Rodeo, L. Fortier, C. Lu, C. Erisken, J. Mao, Protein-releasing polymeric scaffolds induce fibrochondrocyte differentiation of endogenous cells for knee meniscus regeneration in sheep, Sci. Transl. Med. 6 (266) (2014), https://doi.org/10.1126/scitranslmed.3009696, 266ra171.

[37] C. Lee, J. Cook, A. Mendelson, E. Moioli, H. Yao, J. Mao, Regeneration of the articular surface of the rabbit synovial joint by cell homing: a proof of concept study, Lancet (London, England) 376 (9739) (2010) 440–448, https://doi.org/10.1016/s0140-6736(10)60668-x.

[38] I. Motabi, J. DiPersio, Advances in stem cell mobilization, Blood Rev. 26 (6) (2012) 267–278, https://doi.org/10.1016/j.blre.2012.09.003.

[39] I. Winkler, N. Sims, A. Pettit, V. Barbier, J. Nowlan, F. Helwani, I. Poulton, N. van Rooijen, K. Alexander, L. Raggatt, J. Lévesque, Bone marrow macrophages maintain hematopoietic stem cell (HSC) niches and their depletion mobilizes HSCs, Blood 116 (23) (2010) 4815–4828, https://doi.org/10.1182/blood-2009-11-253534.

[40] Z. Sun, J. Liang, X. Dong, C. Wang, D. Kong, F. Lv, Injectable hydrogels coencapsulating granulocyte-macrophage colony-stimulating factor and ovalbumin nanoparticles to enhance antigen uptake efficiency, ACS Appl. Mater. Interfaces 10 (24) (2018) 20315–20325, https://doi.org/10.1021/acsami.8b04324.

[41] C.H. Lee, J.L. Cook, A. Mendelson, E.K. Moioli, H. Yao, J.J. Mao, Regeneration of the articular surface of the rabbit synovial joint by cell homing: a proof of concept study, Lancet 376 (9739) (2010) 440–448, https://doi.org/10.1016/s0140-6736(10)60668-x.

[42] J. Martin, D. McCabe, M. Walter, J. Buckwalter, T. McKinley, N-acetylcysteine inhibits post-impact chondrocyte death in osteochondral explants, J Bone Joint Surg AM 91 (8) (2009) 1890–1897, https://doi.org/10.2106/jbjs.H.00545.

[43] D. Bonasia, A. Marmotti, A. Massa, A. Ferro, D. Blonna, F. Castoldi, R. Rossi, Intra- and inter-observer reliability of ten major histological scoring systems used for the evaluation of in vivo cartilage repair, Knee Surg Sport Tr A 23 (9) (2015) 2484–2493, https://doi.org/10.1007/s00167-014-2975-8.

[44] K. Gelse, D. Riedel, M. Pachowsky, F. Hennig, S. Trattnig, G. Welsch, Limited integrative repair capacity of native cartilage autografts within cartilage defects in a sheep model, J. Orthop. Res. 33 (3) (2015) 390–397, https://doi.org/10.1002/jor.22773, official publication of the Orthopaedic Research Society.

[45] S. Grogan, S. Miyaki, H. Asahara, D. D'Lima, M. Lotz, Mesenchymal progenitor cell markers in human articular cartilage: normal distribution and changes in osteoarthritis, Arthritis Res. Ther. 11 (3) (2009) R85, https://doi.org/10.1186/ar2719.

[46] R. Williams, I. Khan, K. Richardson, L. Nelson, H. McCarthy, T. Analbelsi, S. Singhrao, G. Dowthwaite, R. Jones, D. Baird, H. Lewis, S. Roberts, H. Shaw, J. Dudhia, J. Fairclough, T. Briggs, C. Archer, Identification and clonal characterisation of a progenitor cell sub-population in normal human articular cartilage, PLoS One 5 (10) (2010) e13246, https://doi.org/10.1371/journal.pone.0013246.

[47] G. Dowthwaite, J. Bishop, S. Redman, I. Khan, P. Rooney, D. Evans, L. Haughton, Z. Bayram, S. Boyer, B. Thomson, M. Wolfe, C. Archer, The surface of articular cartilage contains a progenitor cell population, J. Cell Sci. 117 (2004) 889–897, https://doi.org/10.1242/jcs.00912.

[48] M. Murphy, L. Koepke, M. Lopez, X. Tong, T. Ambrosi, G. Gulati, O. Marecic, Y. Wang, R. Ransom, M. Hoover, H. Steininger, L. Zhao, M. Walkiewicz, N. Quarto, B. Levi, D. Wan, I. Weissman, S. Goodman, F. Yang, M. Longaker, C. Chan, Articular cartilage regeneration by activated skeletal stem cells, Nat. Med. 26 (10) (2020) 1583–1592, https://doi.org/10.1038/s41591-020-1013-2.

[49] Y. Wei, L. Luo, T. Gui, F. Yu, L. Yan, L. Yao, L. Zhong, W. Yu, B. Han, J. Patel, J. Liu, F. Beier, L. Levin, C. Nelson, Z. Shao, L. Han, R. Mauck, A. Tsourkas, J. Ahn, Z. Cheng, L. Qin, Targeting cartilage EGFR pathway for osteoarthritis treatment, Sci. Transl. Med. 13 (576) (2021), https://doi.org/10.1126/scitranslmed.abb3946.

[50] M. Murakami, H. Horibe, K. Iohara, Y. Hayashi, Y. Osako, Y. Takei, K. Nakata, N. Motoyama, K. Kurita, M. Nakashima, The use of granulocyte-colony stimulating factor induced mobilization for isolation of dental pulp stem cells with high regenerative potential, Biomaterials 34 (36) (2013) 9036–9047, https://doi.org/10.1016/j.biomaterials.2013.08.011.

[51] I. Khan, R. Williams, C. Archer, One flew over the progenitor's nest: migratory cells find a home in osteoarthritic cartilage, Cell Stem Cell 4 (4) (2009) 282–284, https://doi.org/10.1016/j.stem.2009.03.007.

[52] D. Shi, X. Xu, Y. Ye, K. Song, Y. Cheng, J. Di, Q. Hu, J. Li, H. Ju, Q. Jiang, Z. Gu, Photo-cross-linked scaffold with kartogenin-encapsulated nanoparticles for cartilage regeneration, ACS Nano 10 (1) (2016) 1292–1299, https://doi.org/10.1021/acsnano.5b06663.

[53] P. Chen, S. Zhu, Y. Wang, Q. Mu, Y. Wu, Q. Xia, X. Zhang, H. Sun, J. Tao, H. Hu, P. Lu, H. Ouyang, The amelioration of cartilage degeneration by ADAMTS-5 inhibitor delivered in a hyaluronic acid hydrogel, Biomaterials 35 (9) (2014) 2827–2836, https://doi.org/10.1016/j.biomaterials.2013.12.076.

[54] S. Jia, T. Zhang, Z. Xiong, W. Pan, J. Liu, W. Sun, In vivo evaluation of a novel oriented scaffold-BMSC construct for enhancing full-thickness articular cartilage repair in a rabbit model, PLoS One 10 (12) (2015) e0145667, https://doi.org/10.1371/journal.pone.0145667.

[55] Z. Luo, J. Jiang, Y. Xu, H. Li, W. Xu, S. Wu, Y. Wang, Z. Tang, Z. Lv, L. Yang, Mechano growth factor (MGF) and transforming growth factor (TGF)-β3 functionalized silk scaffolds enhance articular hyaline cartilage regeneration in

rabbit model, Biomaterials 52 (2015) 463–475, https://doi.org/10.1016/j. biomaterials.2015.01.001.

[56] R. Dahlin, L. Kinard, J. Lam, C. Needham, S. Lu, F. Kasper, A. Mikos, Articular chondrocytes and mesenchymal stem cells seeded on biodegradable scaffolds for the repair of cartilage in a rat osteochondral defect model, Biomaterials 35 (26) (2014) 7460–7469, https://doi.org/10.1016/j.biomaterials.2014.05.055.

[57] H. Chen, A. Chevrier, C. Hoemann, J. Sun, V. Lascau-Coman, M. Buschmann, Bone marrow stimulation induces greater chondrogenesis in trochlear vs condylar cartilage defects in skeletally mature rabbits, Osteoarthritis Cartilage 21 (7) (2013) 999–1007, https://doi.org/10.1016/j.joca.2013.04.010.